IMPACT OF BN ADDITIVE ON THERMOELECTRIC PERFORMANCE OF $EuBa_2Cu_3O_y$ SUPERCONDUCTOR

G. Mumladze*, V. Zhghamadze, I. Kvartskhava, N. Margiani

Institute of Cybernetics, Georgian Technical University, Tbilisi, Georgia
**e-mail: g.mumladze@gtu.ge*

Received 06.02.2025
Accepted 21.04.2025

***Abstract**: The thermoelectric phenomenon in the reference (pristine) and BN-added $EuBa_2Cu_3O_y$ high-temperature superconductors has been studied. A series of 4 compounds was prepared by the solid-phase synthesis method. The phase evolution of the prepared materials was analyzed by XRD, and the SEM/EDX technique was employed to investigate the microstructure and elemental composition of the specimens. The temperature dependence of resistivity (ρ) and Seebeck coefficient (S) was measured in the range of 300–1000 K. Power factor (PF) values were calculated for this temperature area. BN addition led to an enhancement of the PF at 973 K from 0.053 mW/m·K² for the reference sample to 0.075 mW/m·K² for the 0.15 wt.% BN-added $EuBa_2Cu_3O_y$.*
***Keywords:** thermoelectricity, $EuBa_2Cu_3O_y$ superconductor, BN additive, power factor.*

Introduction

The increasing impact of global warming on the environment compels scientists to develop various alternatives to fossil fuels, including waste-heat-to-energy conversion technologies. The growing popularity of thermoelectric materials, which can convert part of waste heat into electrical power, is driven by the Seebeck effect [1-2]. The thermoelectric conversion efficiency of materials is determined by the dimensionless figure-of-merit $ZT = S^2T/\rho k$, with S, T, ρ, and k representing the Seebeck coefficient, absolute temperature, electrical resistivity, and thermal conductivity, respectively. The power factor $PF = S^2/\rho$ is an electrical component of the ZT formula that assesses output electrical power [3]. The presence of toxic elements such as tellurium (Te), antimony (Sb), and lead (Pb) in the traditional state-of-the-art intermetallic thermoelectric alloys [4-6] reduces their appeal for large-scale applications. As a result, non-toxic and environmentally friendly alternatives have gained attractiveness in recent years. The discoveries of complex cobalt oxides, such as $NaCo_2O_4$, $Ca_3Co_4O_9$ and $Bi_2M_2Co_2O_x$ (M = Ca, Sr, or Ba), opened the way to the systematic exploration and development of polycrystalline cobaltites for potential applications [7-10]. Layered *p*-type thermoelectric cobalt oxides and layered *p*-type superconducting copper oxides reveal a marked structural resemblance, suggesting that the underlying physics in both structures might be similar [11-13]. Crystallographically, superconducting cuprates and thermoelectric cobaltites are composed of two different layers: electrically insulating blocking ("charge reservoir") and conducting (CuO_2 and CoO_2, respectively) layers. From the charge reservoir layers, holes are doped into the conducting layers. Interestingly, the previously unknown thermoelectric Bi-Sr-Co-O phase was first prepared with the intention to get an analogue of the superconducting Bi-Sr-Ca-Cu system in which the CuO_2 planes have been completely replaced by CoO_2 planes [14]. This resemblance has significant implications for materials science, as it may lead to the development of novel materials with desirable properties. More research is necessary to understand the similarities between these two types of oxides and to uncover new insights into the underlying physics of these materials.

The study of thermoelectric phenomena in the high-temperature superconducting cuprates is currently in its initial stage. There is very little data available on the thermoelectric characteristics of cuprate superconductors above room temperature. It was reported that $Bi_{0.5}Na_{0.5}TiO_3$-added $DyBa_2Cu_3O_y$ superconductor showed the power factor value of PF= 0.036 mW/m·K^2 [15]. A power factor of 0.065 mW/m·K^2 was observed at 773 K for $Pr_{1.06}Ba_{1.94}Cu_3O_y$ composition [16].

Consequently, the RE(Rare-Earth)123 system presents itself as a promising candidate for thermoelectric applications.

In this paper, we studied the impact of boron nitride (BN) additives on the phase evolution, microstructure, and electrical transport properties of the $EuBa_2Cu_3Oy$ superconductor. Then, the power factors of the prepared materials were calculated using the measured temperature dependence of the resistivity and Seebeck coefficient.

Experimental part

Samples with nominal compositions of $EuBa_2Cu_3O_y$ (reference), EuBa2Cu3Oy + 0.1 wt. % BN, $EuBa_2Cu_3O_y$ + 0.15 wt. % BN, and $EuBa_2Cu_3O_y$ + 0.2 wt. % BN were prepared using the solid-state reaction method. The commercially available Eu_2O_3, $BaCO_3$, and CuO precursors, in appropriate molar amounts, were used to prepare four equal batches of $EuBa_2Cu_3O_y$ (reference) material. These powder mixtures were thoroughly ground in a mortar and then transferred to the Fritch Pulverisette 7 Premium Line planetary mill, where they were homogenized for 1 hour at 100 rpm. Afterward, the homogenized powders were calcined stepwise at 1123 K, 1173 K, and 1203 K for a total of 35 hours, with intermediate grinding in an agate mortar. Submicron-sized (~0.2-0.4 μm) BN particles were added in 0, 0.1, 0.15, and 0.2 wt.% to the four equal batches of $EuBa_2Cu_3O_y$. These batches were additionally homogenized at 150 rpm for 1 hour. Then, these powders were pressed into pellets, 10 mm in diameter, under a hydrostatic pressure of 220 MPa. The pellets were sintered at 1223 K in an ambient atmosphere for 35 hours and then cooled to room temperature inside the furnace. After the pellets were cooled, the post-annealing oxygen enrichment procedure was performed: the pellets of four series were heat-treated at 873 K for 4 hours, then at 723 K for an additional 30 hours.

The resistivity as a function of temperature in the range from room temperature to 973 K was measured using the standard four-probe method. The phase evolution was observed by X-ray diffraction using a Dron–3M diffractometer (CuKα radiation). The microstructure and elemental composition were analyzed using a scanning electron microscope (SEM, VEGA TS5130MM) combined with an energy dispersive X-ray (EDX) microanalysis system (INCA Energy 300). The temperature dependence of the resistivity $\rho(T)$ and Seebeck coefficient $S(T)$ was measured simultaneously from room temperature to 973 K using a custom-built setup equipped with a KEITHLEY DMM6500 multimeter. Electrical transport measurements were conducted on bar-shaped samples with dimensions of ~13×7×2.5 mm^3.

Results and discussion

The XRD patterns of the $EuBa_2Cu_3O_y$ + x wt.% (x = 0, 0.1, 0.15, 0.2 BN) series are shown in Fig. 1.

XRD patterns are consistent with previously reported results [17, 18]. No recognizable boron-related diffraction peaks are observed due to the low concentration of BN. Fig. 2 displays SEM micrographs of the surface morphology of prepared materials. The samples consist of small and large grains with sizes of up to several tens of microns. The results of the elemental analysis evidence that the reference sample is homogeneous. The 0.1 wt.% and 0.15 wt.% BN-added $EuBa_2Cu_3O_y$ samples contain small amounts of Ba- and Cu-related secondary phases. The 0.2 wt.% BN-added $EuBa_2Cu_3O_y$ sample is similar to the reference sample in terms of homogeneity.

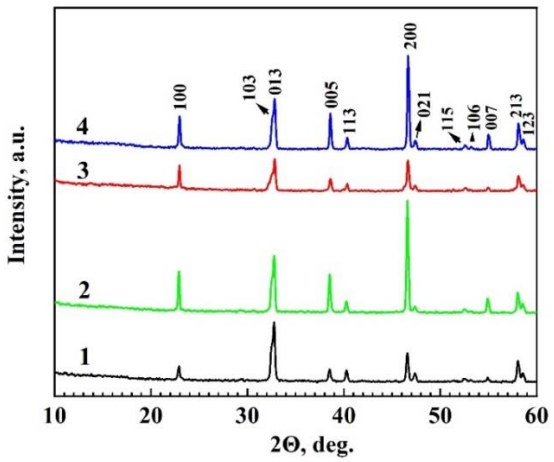

Fig. 1. The XRD patterns of $EuBa_2Cu_3O_y$ + x wt.% BN samples. **1** - x=0; **2** - x=0.1; **3** - x=0.15; **4** - x=0.2

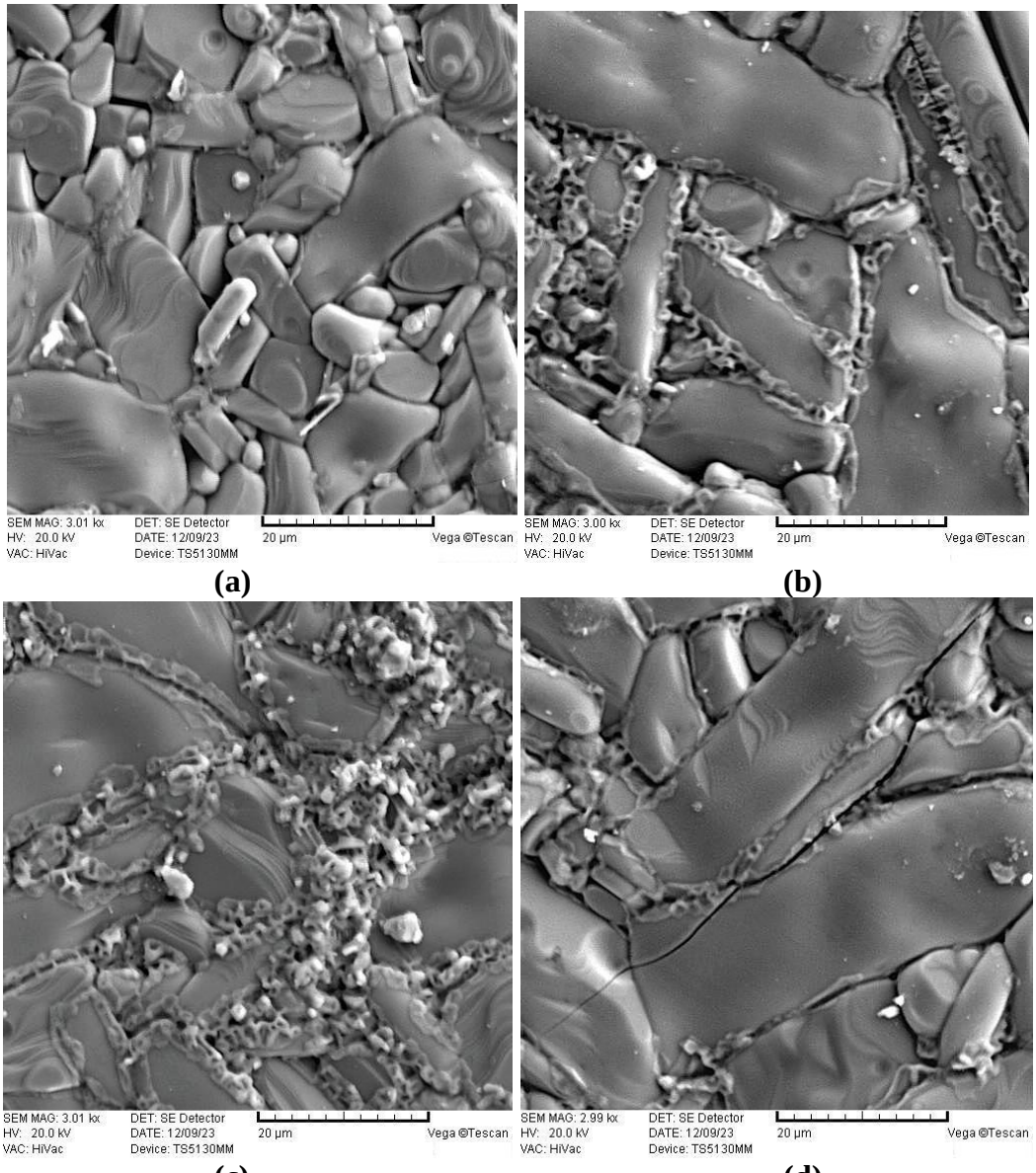

Fig. 2. The SEM images of $EuBa_2Cu_3O_y$ + x wt.% BN materials. **(a)** – x=0; **(b)** 2 – x=0.1; **(c)** – x=0.15; **(d)** – x=0.2

Fig. 3 illustrates the temperature dependence of the resistivity in the prepared materials. The incorporation of BN into the $EuBa_2Cu_3O_y$ causes a steady rise in resistivity above 900 K, which negatively impacts the value of the *PF*, but, as will be seen later, this increase in ρ is compensated by an increase in the Seebeck coefficient.

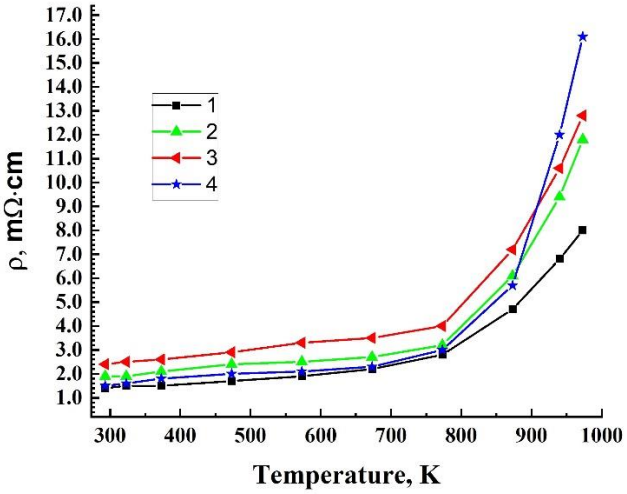

Fig. 3. The resistivity vs temperature dependence of $EuBa_2Cu_3O_y$ + x wt.% BN materials. **1** – x=0; **2** – x=0.1; **3** – x=0.15; **4** – x=0.2.

Fig. 4 illustrates the temperature dependence of the Seebeck coefficient. *S* values increase sharply as the temperature rises above 700 K. Such behavior of *S* indicates the *p*-type conductivity in all samples. BN additive leads to more than a 50% enhancement of the Seebeck coefficient as compared to the reference sample.

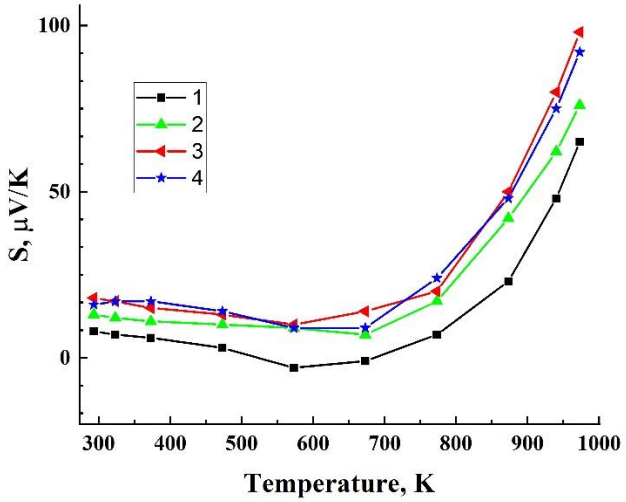

Fig. 4. Temperature dependence of Seebeck coefficient in $EuBa_2Cu_3O_y$ + x wt.% BN materials. **1** – x=0; **2** – x=0.1; **3** – x=0.15; **4** – x=0.2

Using the measured experimental values of the Seebeck coefficient and electrical resistivity, the power factor, $PF = S^2/\rho$ was calculated, as shown in Fig. 5. BN-added compositions possessed higher resistivity compared to the reference sample (see Fig. 3). However, the significantly increased Seebeck coefficients govern the values of the *PF*. The maximum *PF* achieved in the 0.15 wt % BN-added $EuBa_2Cu_3O_y$ (0.075 mW/m·K², at 973 K) is approximately 42% higher than that of the reference $EuBa_2Cu_3O_y$.

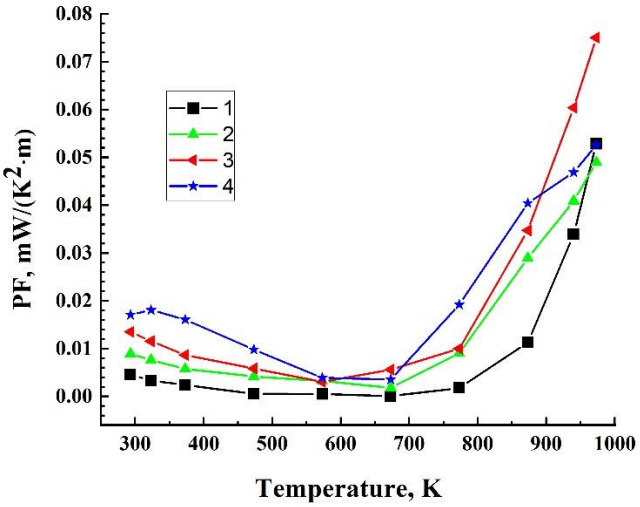

Fig. 5. The temperature dependence of power factor (*PF*) in $EuBa_2Cu_3O_y$ + x wt % BN materials. **1** – x=0; **2** – x=0.1; **3** – x=0.15; **4** – x=0.2

Conclusion

In this study, reference and BN-added $EuBa_2Cu_3O_y$ materials were synthesized using the solid-state reaction method, and the influence of the BN additive on phase evolution, microstructure, elemental composition, and power factor was investigated. BN addition results in a power factor of 0.075 mW/m·K² for the 0.15 wt.% BN-added Eu-123 superconductor at 973 K, which is 1.4 times higher than that of the BN-free $EuBa_2Cu_3O_y$. The increased *PF* observed in this study is comparable to values reported for thermoelectric cobaltites. With further optimization, Eu-123-based materials might provide considerable potential for thermoelectric applications.

Acknowledgment

This research was supported by Shota Rustaveli National Science Foundation of Georgia (SRNSFG) [grant number YS-22-175, Impact of BN and TiN nanoinclusions on the microstructure and superconducting properties of Y(LRE)$Ba_2Cu_3O_y$ HTSs (LRE= Sm and Eu)].

Conflict of interest statement

The authors declare that there are no conflicts of interest.

References

1. Forman C., Muritala I.K., Pardemann R., Meyer B. Estimating the global waste heat potential. *Renewable and Sustainable Energy Reviews*, 2016, **Vol. 57**, p. 1568–1579. DOI: 10.1016/j.rser.2015.12.192;
2. Seebeck T.J. Magnetische polarisation der metalle und erze durch temperaturdifferenz. *Ostwalds Klassiker der exakten Wissenschaften*, 1895, **No 70**, urn:oclc:record:1049682994;
3. He J., Liu Y., Funahashi R. Oxide thermoelectrics: the challenges, progress, and outlook. *Journal of Materials Research*, 2011, **Vol. 26**, p. 1762–1772, DOI: 10.1557/jmr.2011.108;
4. Mammadli P.R., Babanly D.M. Powder X-Ray diffraction study of the Cu_3SbS_3-CuI System. *Chemical Problems*. 2023, **Vol. 21(1)**, p. 57-63. DOI: 10.32737/2221-8688-2023-1-57-63
5. Kaur K., Enamullah, Khandy Sh.A., Singh J., Dhiman Sh. Traditional thermoelectric materials and challenges. *Thermoelectricity and Advanced Thermoelectric Materials*. Sawston, United Kingdom. Woodhead Publishing Series in Electronic and Optical Materials. 2021, p. 139-161, DOI: 10.1016/B978-0-12-819984-8.00009-6;

6. Aghazade A.I., Rustamova S.M., Gojayeva I.M., Orujlu E.N., Babanly D.M., Mammadov A.N. Multy-3D modeling of phase diagram of $PbTe$-Bi_2Te_3-Sb_2Te_3 System. *Chemical Problems*. 2023, **Vol. 21(4)**, p. 353-360. DOI: 10.32737/2221-8688-2023-4-353-360;
7. Terasaki I., Sasago Y., Uchinokura K. Large Thermoelectric Power in $NaCo_2O_4$ Single Crystals. *Phys. Rev. B*, 1997, **Vol. 56**, p. R12685–R12687. DOI: 10.1103/PhysRevB.56.R12685
8. Funahashi R., Matsubara I., Ikuta H., Takeuchi T., Mizutani U., Sodeoka S. An Oxide Single Crystal with High Thermoelectric Performance in Air. *Jpn. J. Appl. Phys*, 2000, **Vol. 39**, p. L1127–L1129. DOI: 10.1143/JJAP.39.L1127;
9. Masset C., Michel C., Maignan A., Hervieu M., Toulemonde O., Studer F., Raveau B., Hejtmanek J. Misfit-layered cobaltite with an anisotropic giant magnetoresistance. *Phys. Rev. B*, 2000, **Vol. 62**, p. 166–175. DOI: 10.1103/PhysRevB.62.166;
10. Funahashi R., Matsubara I., Sodeoka S. Thermoelectric properties of polycrystalline materials. *Appl. Phys. Lett*, 2000, **Vol. 76**, p. 2385–2387. DOI: 10.1063/1.126354;
11. Takada K., Sakurai H., Takayama-Muromachi E., Izumi F., Dilanian R.A., Sasaki T. Superconductivity in two dimensional CoO_2 layers. *Nature*, 2003, **Vol. 422**, p. 53-55. DOI: 10.1038/nature01450;
12. Pelloquin D., Maignan A., Hébert S., Martin C., Hervieu M., Michel C., Wang L.B., Raveau B. New Misfit Cobaltites $[Pb0.7A0.4Sr1.9O_3][CoO_2]1.8$ (A= Hg, Co) with Large hermopower. *Chem. Mater.*, 2002, **Vol. 14**, p. 3100-3105, DOI: 10.1021/cm020162p;
13. Tang X., Tritt T.M. Overview of thermoelectric sodium cobaltite: $Na_xCo_2O_4$. *Journal of the South Carolina Academy of Science*, 2013, **Vol. 6(2)**, Article 2, https://scholarcommons.sc.edu/jscas/vol6/iss2/2;
14. Tarascon J.M., Ramesh R., Barboux P., Hedge M.S., Hull G.W., Greene L.H., Giroud M., LePage Y., McKinnon W.R., Waszcak J.V., Schneemeyer L.F. New non-superconducting layered Bi–oxide phases of formula $Bi_2M_3Co_2O_y$ containing Co instead of Cu. *Solid State Commun.*, 1989, V**ol. 71(8)**, p. 663–668. DOI: 10.1016/0038-1098(89)91813-9;
15. Boonsong P., Watcharapasorn A. High-temperature thermoelectric properties of (1-x)DyBCO − xBNT ceramics. *Journal of Asian Ceramic Societies*, 2022, V**ol. 10**, p. 766-778. DOI: 10.1080/21870764.2022.2127505;
16. Prayoonphokkharata P., Amonpattaratkit P., Kosuga A., Watcharapasorn A. Thermoelectric properties of Pr-substituted YBCO ceramics. *Journal of Alloys and Compounds*, 2021, V**ol. 871**, p. 159552. DOI: 10.1016/j.jallcom.2021.159552;
17. Trolio A.D., Grimaldi G., Mattei G., Testa A.M. Structural and superconducting properties of $EuBa_2Cu_3O_{7-x}$ thin films grown by off-axis pulsed laser deposition. *Superconductor Science and Technology*, 2004, **Vol. 17(8)**, p. 1009–1013. DOI: 10.1088/0953-2048/17/8/010;
18. MacManus-Driscoll J.L., Alonso J.A., Wang P.C., Geballe T.H., Bravman J.C. Studies of structural disorder in $ReBa_2Cu_3O_{7-x}$ thin films (Re=rare earth) as a function of rare-earth ionic radius and film deposition conditions. *Physica C*, 1994, **Vol. 232**, p. 288-308. DOI: 10.1016/0921-4534(94)90789-7.